

High pressure phase of RDX

Naoyuki Goto^{**}, Hiroshi Yamawaki^{**}, Kunihiro Wakabayashi^{***},
Yoshio Nakayama^{***}, Masatake Yoshida^{***}, and Mitsuo Koshi^{*}

^{*}Department of Chemical System Engineering, School of Engineering, The University of Tokyo, 7-3-1 Hongo, Bunkyo-ku, Tokyo 113-8656, JAPAN

[†]corresponding author: goto@chemsys.t.u-tokyo.ac.jp

^{**}Research Institute of Instrumentation Frontier, National Institute of Advanced Industrial Science and Technology (AIST), 1-1-1 Higashi, Tsukuba, Ibaraki 305-8565, JAPAN

^{***}Research Center for Explosion Safety, National Institute of Advanced Industrial Science and Technology (AIST), 1-1-1 Higashi, Tsukuba, Ibaraki 305-8565, JAPAN

Received: March 3, 2005 Accepted: May 25, 2005

Abstract

We have studied behaviors of one of high sensitive explosives, RDX (hexahydro-1,3,5-trinitro-1,3,5-triazine), under static ultrahigh pressures (up to 50 GPa) generated by a diamond anvil cell (DAC) with FT-IR spectroscopy. Quantum chemical calculations using a density functional theory (DFT) with the Becke3-Lee-Yang-Parr (B3LYP) hybrid density functional and 6-31G(d), 6-311+G(d,p), and 6-311++G(3df,3pd) basis sets were also performed on six conformers of RDX. The molecular structure of high pressure phase of RDX (γ -RDX) was discussed by comparing the shape of the FT-IR spectra with the shape obtained by DFT calculations. Potential energy surface (PES) calculations were performed to discuss the validity of the isomerization. Molecular dynamics (MD) simulations were performed to discuss the pressure dependence of the IR frequencies.

High pressure FT-IR spectra did not show degenerated structures which are characteristics of C_{3v} point group. Comparing the observed FT-IR spectra, IR frequencies obtained by DFT, and the pressure dependence of the IR frequencies obtained by MD simulations, the high pressure structure of RDX was suggested to be of the AEE type, in which one of the NO_2 bond angles to the six-membered ring is axial, while the others are equatorial. PES calculations also supported this conclusion.

1. Introduction

Explosion of energetic materials is a less understood phenomenon, in terms of the mechanism of its initiation of reaction. Recent advances in computer technologies, density functional theory (DFT) and molecular dynamics (MD) simulations have allowed the computational study of crystals. Hexahydro-1,3,5-trinitro-1,3,5-triazine (RDX) is a prototype of explosives to investigate the explosion mechanism.^{1)–13)} Calculations need atomic coordinates of the crystal, however, the crystal structure of high pressure phase of RDX (γ -RDX) which has a phase transition point at about 4 GPa at room temperature has not yet clarified. Its ambient pressure phase (α -RDX) had been first investigated by Hultgren¹⁴⁾ and refined on the basis of single-crystal neutron-diffraction data.¹⁵⁾ The crystal structure of the α -RDX is known to be orthorhombic, with 8 molecules per unit cell, and its space group is $Pbca$. The molecular

structure of the α -RDX represents a chair configuration, and has anomalous bond angles between the nitro groups and the six-membered ring, two of which are axial (A) and the other is equatorial (E), so that the α -RDX molecule belongs to the C_s point group, while the structures in β phase, in solution, and in vapor phase, belong to C_{3v} point group.¹⁶⁾ This experimental fact shows that the energy gap and the barrier between the axial bond and the equatorial bond is small enough to change the molecular structure in ambient conditions, which is supported by the DFT calculations on the isolated RDX molecule.^{10), 11)}

In this work, Fourier transform infrared (FT-IR) absorption spectra were measured under high pressures up to 50 GPa, generated by a diamond anvil cell (DAC) and DFT frequency calculations were performed on six configurations, and both were compared to discuss the molecular structure of the γ -RDX. Six configurations include five

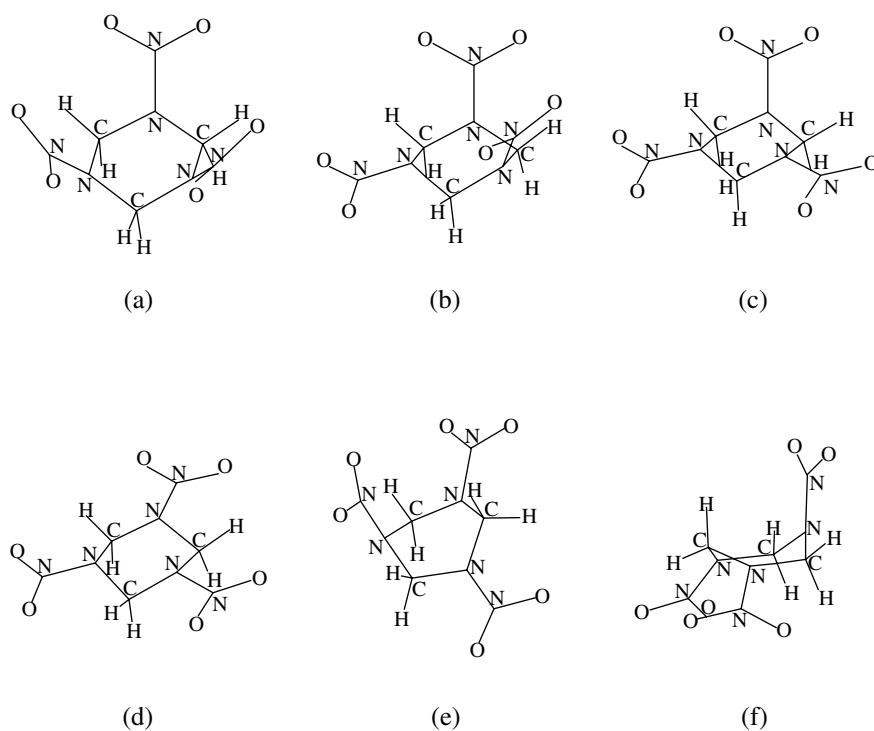


Fig. 1 Candidates of RDX conformers. (a) C_{3v} AAA, (b) C_s AAE, (c) C_s AEE, (d) C_{3v} EEE, (e) C_1 twist, (f) C_s boat.

chair conformations, C_{3v} AAA, C_s AAE, C_s AEE, C_{3v} EEE, and C_1 twist and a C_s boat conformation, named C_s boat. Molecular structures of these conformers are shown in Fig. 1. Two potential energy surface (PES) on the angle and the bond length between an NO_2 group and the six-membered ring were also calculated by DFT, to discuss the possibility of transformation from the AAE conformer to the AEE conformer under high pressures. Pressure dependence of the IR peak positions were compared with the results of molecular dynamics (MD) simulations.

2. Experimental section

2.1 Diamond anvil cells

Static pressures up to several hundreds GPa can be generated by using diamond anvil cells (DACs).¹⁷⁾ We used diamonds of a head diameter of 0.3 mm with a height of 1.5 mm, and metallic gasket of iron (PK) or stainless alloy (SUS-301). This apparatus can generate high pressures up to around 50 GPa.

A small ruby ball with a diameter of 10 μm was placed together with the sample. The pressure was evaluated from the shift of ruby fluorescence wavelength of R_1 line (694.24 nm at ambient pressure) by applying Mao's equation¹⁸⁾,

$$P = 1904 \times ((\lambda/\lambda_0)^5 - 1) / 5, \quad (1)$$

where P is the pressure in GPa, λ is the wavelength of a ruby fluorescence, and λ_0 is that at ambient pressure.

2.2 FT-IR measurement

The optical openings of the DAC were 60° for both incident and transmitted infrared light, matching well those of

the microfocusing optics of an FT-IR spectrometer. Transmission infrared spectra were taken for about area, which is tunable, of the specimen with a microscope FT-IR spectrometer having MCT detector (JASCO FT/IR-550 combined with an infrared microscope MH-11). The spectral resolution was set to 1 cm^{-1} and the number of accumulations to 512. FT-IR spectra were obtained by dividing the measured raw spectra by the reference spectrum of the empty DAC. Cesium iodide (CsI) or potassium bromide (KBr) was placed with the sample as a pressure medium, which also functions to avoid saturations of IR spectra by reducing the thickness of the sample.

3. Computational methods

3.1 Quantum chemical calculations

Quantum chemical calculations were performed to investigate the molecular structure of γ -RDX. The molecular geometry optimizations followed by normal mode analyses were performed on each isolated molecule of six conformers as the candidates for the γ -RDX molecule. We will later discuss the molecular structure of γ -RDX by comparing the FT-IR spectra and the normal mode frequencies obtained by quantum chemical calculations. All calculations were carried out with GAUSSIAN 03 program package.¹⁹⁾ All geometry optimization and frequency calculations used a density functional theory (DFT) with the Becke3-Lee-Yang-Parr (B3LYP) hybrid density functional and 6-31G(d), 6-311+G(d,p), and 6-311++G(3df,3pd) basis sets. Calculated vibrational frequencies were scaled by 0.9613, which is a scaling factor suitable for frequencies obtained by the B3LYP/6-31(d) level of theory.²⁰⁾

The potential energy changes on the angle and the bond length between an NO_2 group and the six-membered ring

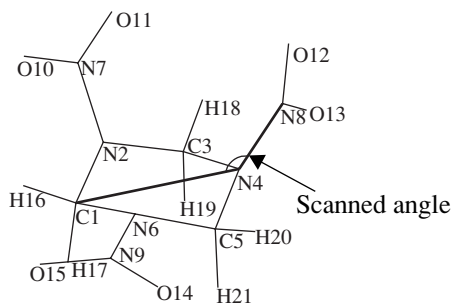


Fig. 2 The angle scanned in the PES calculation of the AAE conformer in this work is indicated. The angle is measured in the upper side in this figure, so that this angle is 125° .

were calculated as a function of N8-N4-N1 angle (see Fig. 2) varied by 1° step and N8-N4 bond length varied by 0.01 \AA step at the B3LYP/6-31G(d) level of theory. We will later discuss the validity of the isomerization from the α phase structure to the assumed γ phase structure by these potential energy surface (PES) calculations. In these calculations, the AAE optimized structure was used as the reference structure.

3.2 Molecular dynamics simulations

Molecular dynamics (MD) simulations were performed to investigate the pressure effects on the vibrational frequencies, which could not be discussed only by the calculations on isolated molecules described above. In these MD simulations, molecular structures are retained by intramolecular potentials set. Intermolecular potentials set was used which play an important role in reproducing the environments of pressurized solid. IR frequencies in various pressures will be later discussed by comparing the FT-IR spectra with the MD simulations. All MD simulations were carried out with General Utility Lattice Program²¹⁾ (GULP) which simulates solid properties under various pressures taking both intramolecular and intermolecular atomic forces into account. A flexible potential was used to calculate the vibrational frequencies of the AEE conformer crystal at the pressure ranging from 0 to 50 GPa. The total potential V_{total} is described as the sum of intra- and intermolecular potentials. The intermolecular potential consists of the superposition of a pairwise sum of Buckingham (6-exp, repulsion and dispersion) and coulombic potentials V^C of the form:

$$V_{\alpha\beta}(r_{\alpha\beta}) = A_{\alpha\beta} \exp(-B_{\alpha\beta} r_{\alpha\beta}) - \frac{C_{\alpha\beta}}{r_{\alpha\beta}^6}, \quad (2)$$

and,

$$V_{\alpha\beta}^C(r_{\alpha\beta}) = \frac{q_\alpha q_\beta}{4\pi\epsilon_0 r_{\alpha\beta}}, \quad (3)$$

where $r_{\alpha\beta}$ is the interatomic distance between the atoms α and β belonging to different molecules, q_α and q_β are the

Table 1 Atom-atom Buckingham potential parameters of α -RDX.

pair (α - α)	$A_{\alpha\alpha}$ (kJ mol ⁻¹)	$B_{\alpha\alpha}$ (\AA)	$C_{\alpha\alpha}$ (kJ mol ⁻¹ \AA^{-6})
H-H	9213.510	3.74	136.3800
C-C	369726.330	3.60	2439.3459
N-N	264795.246	3.78	1668.3316
O-O	290437.820	3.96	1453.3114

corresponding electrostatic charges on these atoms, and ϵ_0 is the dielectric constant. The parameters $A_{\alpha\beta}$, $B_{\alpha\beta}$, and $C_{\alpha\beta}$ for different types of atomic pairs in α -RDX crystal have been previously published by Sorescu *et al.*¹⁾ and have been used in this work. Similar calculations have been performed by Ye *et al.*²²⁾ on PETN. The values of these intermolecular potential parameters are given in Table 1. $A_{\alpha\beta}$, $B_{\alpha\beta}$, and $C_{\alpha\beta}$ are calculated by using traditional combination rules to obtain the heteroatom parameters from homoatom parameters:

$$\begin{aligned} A_{\alpha\beta} &= \sqrt{A_{\alpha\alpha} A_{\beta\beta}} \\ B_{\alpha\beta} &= (B_{\alpha\alpha} + B_{\beta\beta})/2, \\ C_{\alpha\beta} &= \sqrt{C_{\alpha\alpha} C_{\beta\beta}} \end{aligned} \quad (4)$$

The set of partial charges used in the α -RDX simulation were determined by CHelpG keyword of Gaussian 94 program package in which electronic structure calculations were performed at the MP2/6-31G(d,p) level¹⁾. On the other hand, Mulliken atomic charges were used for the AEE conformer as a candidate of the γ -RDX crystal.

The intramolecular potentials were assumed to have the form as follows:

$$V_{intra} = \sum V_{bond} + \sum V_{angle} + \sum V_{torsion} + \sum V_{nonbonded}, \quad (5)$$

to describe the bond stretching (V_{bond}), angle bending (V_{angle}), torsional motions ($V_{torsion}$) and nonbonded ($V_{nonbonded}$) interactions that occur within an individual molecule.

The covalent bond stretch can be approximated as a harmonic oscillator,

$$V_{bond} = \frac{1}{2} k_r (r - r_0)^2, \quad (6)$$

where r is the bond distance, r_0 is the equilibrium bond length and k_r is the force constant describing the stiffness of the bond.

The angle-bending potential is represented by the form,

$$V_{angle} = \frac{1}{2} k_\theta (\theta - \theta_0)^2, \quad (7)$$

where k_θ is the force constant and θ_0 is the equilibrium angle.

The torsional potential is represented by the form,

$$V_{torsion} = V_\phi (1 + i \cos(m(\Phi - \Phi_0))), \quad (8)$$

where V_ϕ is a half of the intramolecular torsional barrier, Φ is the torsional angle, and $m=1, 2, 3$, or 4 , and i is $+1$ or -1 according to the sign of m phase. Nonbonded interactions are considered intramolecularly for all atoms separated by three or more bonds in RDX molecules. The potential is represented by the Lennard-Jones form,

$$V_{\alpha\beta}^{LJ}(r_{\alpha\beta}) = Ar_{\alpha\beta}^{-12} - Br_{\alpha\beta}^{-6}, \quad (9)$$

where $r_{\alpha\beta}$ is the distance between atoms α and β .

All force-field parameters in expressions (6)-(9) are adopted by the earlier literature²³⁾ on simulations of proteins and nucleic acids which are given in Table 2.

4. Results and discussion

4.1 Phase transition

The room-temperature-stable orthorhombic form is known as α -RDX with the space group of $Pbca$. α -RDX is also known to undergo a phase transition into high-pressure phase γ -RDX at approximately 4.0 GPa at room temperature with a 1.6% reduction in volume.²⁴⁾ Figure 3

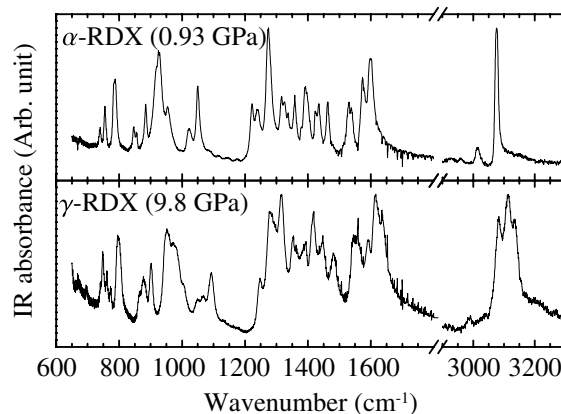


Fig. 3 FT-IR spectra of α -RDX (top, at 0.93 GPa) and γ -RDX (bottom, at 9.8 GPa), respectively.

shows the infrared spectra of RDX at 0.93 GPa (top) and at 9.8 GPa (bottom), respectively. The number of CH_2 stretching modes with strong intensities above 3000 cm^{-1} is three at 9.8 GPa, whereas it is one at 0.93 GPa. Similarly in the N-N modes region, the number of strong modes is one in 0.93 GPa (at 1214 cm^{-1}), but becomes two in 9.8 GPa (at 1279 cm^{-1} and 1314 cm^{-1}). These differences of spectral shapes ensure the phase transition from α phase to γ phase and imply a possibility of a molecular structural

Table 2 The force constants of the intramolecular potential parameters for RDX.

bond stretching parameters			angle bending parameters		
bond	k_r ($\text{kJ mol}^{-1} \text{ \AA}^{-2}$)	r_0 (\AA)	angle	k_θ ($\text{kJ mol}^{-1} \text{ rad}^{-2}$)	θ (deg)
C-N	2716.99	1.454	C-N-C	793.28	109.50
N-N	2914.91	1.380	N-C-N	608.09	109.50
N-O	3123.77	1.210	C-N-N	969.26	125.25
C-H	2998.09	1.081	N-O-N	1008.84	117.20
			O-N-O	859.77	125.60
			N-C-H	243.83	109.50
			H-C-H	235.07	109.33
four-body potential parameters					
dibedral angle	V_ϕ (kJ mol^{-1})	m	i		
C-N-N-O	8.68	2	-1		
C-N-C-N	14.5	1	-1		
nonbonded potential			$V_{\alpha\beta}^{LJ}(r_{\alpha\beta}) = Ar_{\alpha\beta}^{-12} - Br_{\alpha\beta}^{-6}$		
pair	A (eV \AA^{12})	B (eV \AA^6)	pair	A (eV \AA^{12})	B (eV \AA^6)
N2-N4	14392.4	12.441	C1-N4	20542.7	12.3967
N4-N6	14392.4	12.441	C3-N6	20542.7	12.3967
N6-N2	14392.4	12.441	C5-N1	20542.7	12.3967
O-O*	144.677	0.22403			

*O-O pair in different NO_2 group only.

change between these phases.

The pressure hydrostaticity in the DAC dwindled with increasing the pressure, so that the ruby fluorescence spectra broadened and the differences among the peak wavelengths of ruby chips in the DAC gradually. Pressure distributions caused a vague spectral change at the phase transition point, which is essentially supposed to show a distinct change under a hydrostatic compression. Although there are pressure distributions whole of the sample could be said as γ -RDX at 9.8 GPa by two reasons. One is that the peak width of each ruby fluorescence was not so large that a pressure of a part of the sample is less than 4 GPa. The other is that the fluorescence peak wavelengths of several ruby chips in the DAC did not show large differences.

4.2 IR peak pattern of γ -RDX

The molecular and crystal structures of the γ -RDX are less understood. In this work, its molecular structure was discussed by comparing the IR spectra of γ -RDX with the frequencies calculated by DFT. Frequency patterns of five candidate conformers C_{3v} AAA, C_s AAE, C_s AEE, C_{3v} EEE, and C_1 twist calculated at the B3LYP/6-311++G(3df,3pd) level of theory are shown in Fig. 4, which are drawn by convoluting a Lorentz line shape with full width at half maximum (FWHM) of 10 cm^{-1} for all peaks. The FWHM of vibron peaks at room temperature is expected to be around 10 cm^{-1} which is mainly caused by dephasing. The frequencies and the IR intensities of the AAE and the AEE conformers are listed in Tables 3 and 4. Frequency patterns did not show large dependence on the basis set 6-31G(d), 6-311+G(d,p), and 6-311++G(3df,3pd). The C_{3v} AAA and the C_{3v} EEE conformers showed degenerated IR structures caused by the C_{3v} characteristics in the regions 800 ~ 1000 cm^{-1} , 1200 ~ 1300 cm^{-1} , and 1500 ~ 1600 cm^{-1} ,

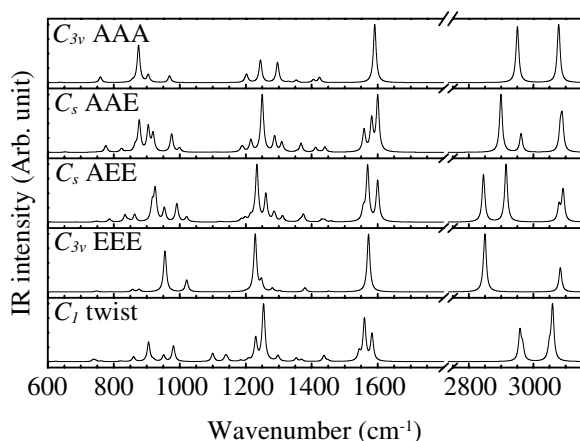


Fig. 4 Calculated frequency patterns of five candidate conformers C_{3v} AAA, C_s AAE, C_s AEE, C_{3v} EEE, and C_1 twist at the B3LYP/6-311++G(3df,3pd) level of theory. For comparison with the spectra, all peaks are drawn with spectral shapes obtained by the convolution with Lorentz functions (FWHM = 10 cm^{-1}). IR intensities of each region 600 ~ 1800 cm^{-1} and 2750 ~ 3150 cm^{-1} were separately normalized to fit into each frame.

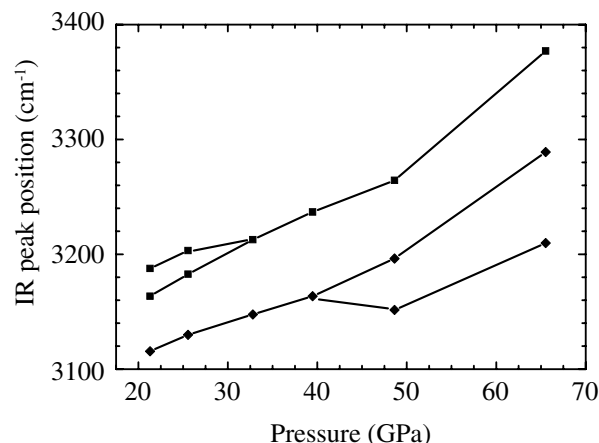


Fig. 5 Experimental pressure dependence of the spectral shifts of the CH_2 stretching modes.

which are different from the non-degenerated spectrum of γ -RDX (Fig. 3). The C_1 twist conformer showed too weak peaks in the region 800 ~ 1000 cm^{-1} and 1300 ~ 1500 cm^{-1} relative to its maximal peak to identify this conformer to be γ -RDX (Fig. 3). The geometry optimization of the C_s boat conformer did not converge to a stable molecule.

Almost all peaks in the spectra showed blue shifts with the increase of the pressure. Figure 5 shows peak shifts of CH_2 stretching modes above 3000 cm^{-1} . In this region, vibrational modes are sparse and peak fitting to a Lorentz functions is rather easy. Peak positions were determined by this peak fitting. A peak splitting of one of the CH_2 stretching modes was observed at between 40 GPa and 50 GPa in Fig. 5. One of these split peaks is supposed to be an infrared inactive mode No. 53 in Table 4, and its infrared activity was changed by the molecular deformation caused by the high pressure.

4.3 Potential energy surface calculations

Two PES calculations at the B3LYP/6-31G(d) level of theory were performed to investigate the validity of the assumption that the molecular structure of γ -RDX is the C_s AEE conformer. Resulting PES as a function of the angle of N8-N4-C1 is shown in Fig. 6. Two local minima are in this figure with 1.368 kcal mol^{-1} difference in energy. The lower minimum corresponds to the optimized AAE conformer and the higher one corresponds to the optimized AEE conformer.

The local maximum between these two local minima, 1.770 kcal mol^{-1} higher than the AAE optimized structure, is the transition state (TS) of the isomerization reaction from the AAE conformer to the AEE conformer. The TS structure and energy were calculated by using higher basis functions, 6-311+G(d,p) and 6-311++G(3df,3pd). These calculations also showed low energy gaps between the TS and the AAE, 1.221 kcal mol^{-1} and 1.039 kcal mol^{-1} respectively. In these calculations zero-point energy corrections were included. These calculations show the fact that the energy gaps among the TS and conformers of AAE and

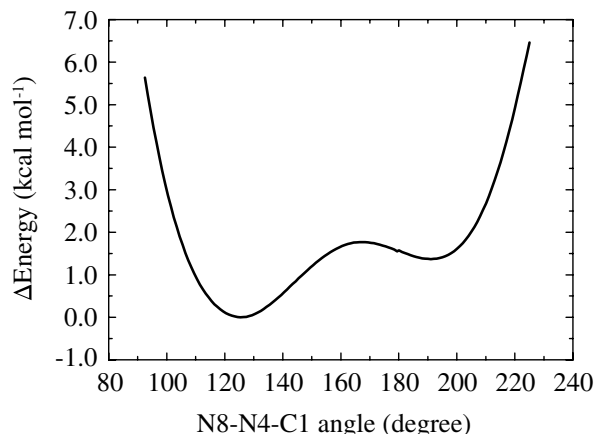


Fig. 6 Potential energy surface scan on the N8-N4-C1 angle at the B3LYP/6-31G(d) level of theory. Energies are expressed as difference between the minimum, which means the optimized geometry of the AAE conformer.

AEE are small enough that these conformers isomerize each other at room temperature when the molecular environment changes. Therefore it is suggested that this isomerization occurs as a result of changes of the crystal field effect, in this case, high pressure.

The PES as a function of the bond length of N8-N4 is shown in Fig. 7. There is a local minimum in the PES where the molecule is the optimized to the AAE structure. In Fig. 7, the change of the N8-N4-C1 angle is also drawn because this angle depends on the N8-N4 bond length. The decrease of the N8-N4 bond length resulted in the increase of the N8-N4-C1 angle, and the molecular structure gradually changed into that of AEE, although the N8-N4 bond length is different. In general, decrease in bond lengths is interpreted as an effect of high pressures in molecules whose vibrational frequencies show blue shifts with increasing pressures. Therefore, this PES calculation may correspond to the molecular structure at high pressures, and the transformation from the AAE to the AEE conformer under high pressure is suggested.

4.4 Assignments of the IR peaks of α -RDX

IR spectra of α -RDX were reported by Karpowicz *et al.*¹⁶⁾, and IR and Raman spectra, by Rey-Lafon *et al.*²⁵⁾ Rice *et al.*¹¹⁾ performed DFT calculations on RDX conformers, and assigned FT-IR spectrum of α -RDX to the AAE conformer and of β -RDX to the AAA conformer. However, the assignments of α -RDX by Rice *et al.* have a discrepancy with the experimental assignments by Rey-Lafon *et al.* in terms of the irreducible representation of 1352 cm^{-1} mode (in this work, 1358 cm^{-1}), which is A' by Rey-Lafon *et al.* but A'' by Rice *et al.*

In this work, the assignments were performed by comparing the FT-IR spectrum at 0.93 GPa and calculated frequencies of AAE conformer at the B3LYP/6-311++G(3df,3pd) level of theory so that each irreducible representation makes consistent with that by Rey-Lafon *et al.* Table 3

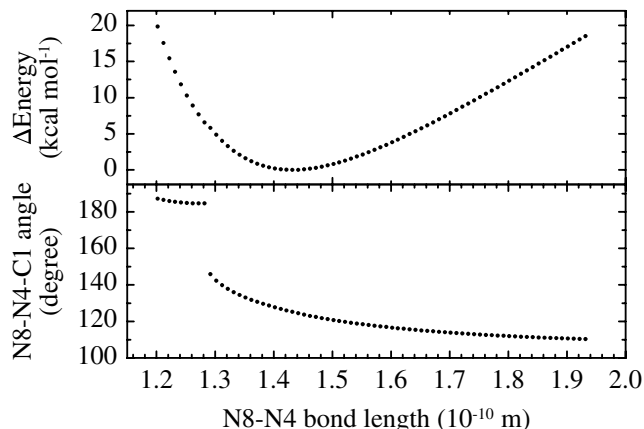


Fig. 7 Potential energy surface scan on the N8-N4 bond length (top) and the N8-N4-C1 angles against the bond lengths (bottom) at the B3LYP/6-31G(d) level of theory.

shows the frequencies both by the calculation and by the FT-IR spectrum with their assignments. Each experimental frequency was determined by reading the wavenumber at which the intensity have its local maximal value, respectively. Vibrational characteristics were assigned by considering the vibrational vectors by the DFT calculation, so that they did not conflict with the assignments by Rey-Lafon *et al.*

4.5 Assignments of the IR peaks of γ -RDX

The structure of the γ -RDX is less understood, and its IR spectra have not yet been assigned. Assignments were performed by assuming the molecular structure of γ -RDX to be the AEE conformer. Table 4 shows the frequencies both by the calculation (B3LYP/6-311++G(3df,3pd)) on the AEE conformer and by the FT-IR spectrum of γ -RDX at 9.8 GPa and their assignments determined by comparing them. Although absolute values of γ -RDX and the AEE conformer do not agree because of blue shifts caused by the increase of the pressures, relative values of the frequencies correspond each other.

4.6 Molecular dynamics simulations

MD simulations were performed under NPT conditions (constant number of particles, pressure, and temperature) at every five GPa from 0 to 50 GPa. The geometry was optimized in fractional coordinates using the intra- and inter-molecular potential parameters described above at each pressure. After the geometry optimization, phonon and vibron frequencies and their infrared intensities are calculated. In these simulations, the initial structure of the γ -RDX molecule at 0 GPa was assumed to be the AEE structure in the crystal which is the same as that of α -RDX, orthorhombic space group of *Pbca* with 8 molecules in a unit cell, $a=13.182$, $b=11.574$, $c=10.709$.¹⁵⁾ At the other pressures, the optimized geometry at the pressure 5 GPa lower than its target pressure was used as the initial geometry.

Table 3 The frequencies and IR intensities of the AAE conformer, calculated at the B3LYP/6-311++G(3df,3pd) level of theory and assignments of the IR spectrum of α -RDX.

AAE calculated by B3LYP/6-311++G(3df,3pd)				α -RDX experiment at 0.93 GPa		
No.	freq. (cm ⁻¹)	IR int.	irr. rep.	freq. (cm ⁻¹)	int.	assignment
1	42.0	0.0222	A''			
2	55.3	2.5093	A'			
3	59.7	1.9647	A'			
4	71.5	0.0104	A''			
5	88.5	0.2144	A''			
6	105.1	0.014	A'			
7	200.3	7.8974	A''			
8	217.3	1.6485	A'			
9	279.0	0.0167	A''			
10	312.9	2.5259	A'			
11	357.8	0.0569	A''			
12	385.7	0.6218	A''			
13	391.9	8.6007	A'			
14	419.8	7.703	A'			
15	444.1	22.0115	A'			
16	557.5	10.4335	A''			
17	568.0	0.5204	A''			
18	587.7	15.5246	A'			
19	629.6	0.3154	A''			
20	652.6	4.5281	A'			
21	735.9	2.2632	A'	738	w	w(NO ₂)
22	742.3	0.0841	A''			
23	751.9	3.1996	A'			
24	775.9	58.6956	A'	755	m	w(NO ₂)
25	823.4	31.6658	A'	787	s	ν_s (ring) and δ (NO ₂)
26	839.2	4.8185	A''	847	w	ν_{as} (NN) and δ (NO ₂)
27	865.1	46.1095	A'	855	w	ring and δ (NO ₂)
28	877.2	269.6733	A''	884	m	ring and δ (NO ₂)
29	904.5	213.313	A'	915	sh	ring and δ (NO ₂)
30	919.0	153.5789	A'	925	s	ρ (CH ₂)
31	975.3	157.2973	A'	954	m	ρ (CH ₂)
32	999.4	35.623	A''	1021	m	ρ (CH ₂)
33	1106.9	2.5641	A''	1050	s	ν_{as} (ring)
34	1186.5	27.1524	A'			
35	1191.1	34.3793	A''			
36	1215.5	97.7278	A'	1223	m	ν_{as} (ring)
37	1218.2	7.416	A''	1238	m	w(CH ₂)
38	1249.7	348.4508	A' }			
39	1250.0	152.5022	A'' }	1273	vs	ν_s (NO ₂) and w(CH ₂)
40	1287.5	134.9601	A'	1316	m	ν_s (NN) and τ (CH ₂)
41	1309.2	79.0783	A'	1358	m	τ (CH ₂)
42	1311.9	4.2691	A''			
43	1322.3	3.5353	A''			
44	1354.9	6.3821	A''	1380	sh	w(CH ₂)
45	1367.7	76.6002	A'	1392	s	w(CH ₂)
46	1411.7	40.9118	A'	1423	m	δ (CH ₂)
47	1425.1	3.7406	A''	1435	s	δ (CH ₂)
48	1440.2	45.5444	A'	1463	s	δ (CH ₂)
49	1558.7	190.9811	A''	1531	s	ν_{as} (NO ₂) and in-plane(NN)
50	1581.7	275.1993	A''	1574	s	ν_{as} (NO ₂) and in-plane(NN)
51	1600.1	484.0363	A'	1601	s	ν_{as} (NO ₂) and in-plane(NN)
52	2898.3	3.1412	A''			
53	2899.5	38.0691	A'			
54	2961.7	13.1093	A'	3014	w	ν_s (CH ₂)
55	3083.4	14.3436	A' }			
56	3088.6	14.4469	A'' }	3076	s	ν_{as} (CH ₂)
57	3090.1	8.5922	A' }			

Table 4 The frequencies and IR intensities of the AEE conformer, calculated at the B3LYP/6-311++G(3df,3pd) level of theory and assignments of the IR spectrum of γ -RDX.

AEE calculated by B3LYP/6-311++G(3df,3pd)				γ -RDX experiment at 9.8 GPa		
No.	freq. (cm ⁻¹)	IR int.	irr. rep.	freq. (cm ⁻¹)	int.	assignment
1	47.4	0.4888	A''			
2	56.4	6.1721	A'			
3	65.3	0.8184	A'			
4	77.4	0.0002	A''			
5	86.0	0.2116	A''			
6	117.2	2.0564	A'			
7	171.0	5.1139	A'			
8	197.8	1.6945	A''			
9	245.6	3.3878	A'			
10	286.6	4.2193	A''			
11	325.2	1.3056	A'			
12	329.1	0.0711	A''			
13	389.4	5.5692	A''			
14	406.3	8.2053	A'			
15	446.8	18.0463	A'			
16	556.2	11.2178	A'			
17	590.6	11.3248	A''			
18	595.9	2.8733	A''			
19	605.7	2.2933	A'			
20	685.7	1.1826	A''			
21	742.3	3.9937	A'			
22	750.0	3.6365	A'			
23	750.4	2.9373	A''			
24	786.8	29.0342	A'			
25	834.1	63.9768	A'	797	s	ν_s (ring) and δ (NO ₂)
26	844.6	15.328	A''	877	m	ν_{as} (NN) and δ (NO ₂)
27	863.3	68.7396	A'	902	s	ring and δ (NO ₂)
28	916.5	155.7932	A'	949	s	ring and δ (NO ₂)
29	925.5	287.811	A''	974	sh	ring and δ (NO ₂)
30	953.3	125.5248	A'	1002	sh	ρ (CH ₂)
31	991.2	167.2622	A''	1053	w	ρ (CH ₂)
32	1020.8	46.508	A'	1069	w	ρ (CH ₂)
33	1123.5	5.0456	A''	1094	m	ν_{as} (ring)
34	1186.5	22.8997	A'			
35	1198.0	33.714	A''			
36	1214.5	47.0383	A'	1248	sh	ν_{as} (ring)
37	1225.6	19.5618	A''			
38	1233.9	518.265	A''	1277	s	ν_s (NO ₂) and w (CH ₂)
39	1261.0	248.4431	A'	1286	sh	ν_s (NO ₂) and w (CH ₂)
40	1285.3	61.9964	A'	1317	vs	ν_s (NN) and τ (CH ₂)
41	1288.5	31.455	A''	1354	s	τ (CH ₂)
42	1311.5	52.9568	A'			
43	1315.7	0.946	A''			
44	1365.3	19.2649	A'	1394	m	w (CH ₂)
45	1374.7	70.2991	A''	1419	s	w (CH ₂)
46	1430.5	22.6698	A''	1447	m	δ (CH ₂)
47	1439.1	20.4949	A'	1484	m	δ (CH ₂)
48	1459.6	8.2894	A'	1560	s	δ (CH ₂)
49	1556.5	102.7068	A''	1591	w	ν_{as} (NO ₂) and in-plane (NN)
50	1569.5	509.0795	A'	1639	s	ν_{as} (NO ₂) and in-plane (NN)
51	1599.9	375.6528	A''	1635	sh	ν_{as} (NO ₂) and in-plane (NN)
52	2845.3	30.6439	A'	3083	m	ν_s (CH ₂)
53	2908.3	0.2234	A''			
54	2915.2	37.3151	A'	3115	s	ν_s (CH ₂)
55	3079.3	10.0499	A'			
56	3091.4	13.8679	A''	3136	m	ν_{as} (CH ₂)
57	3093.1	7.1282	A' }			

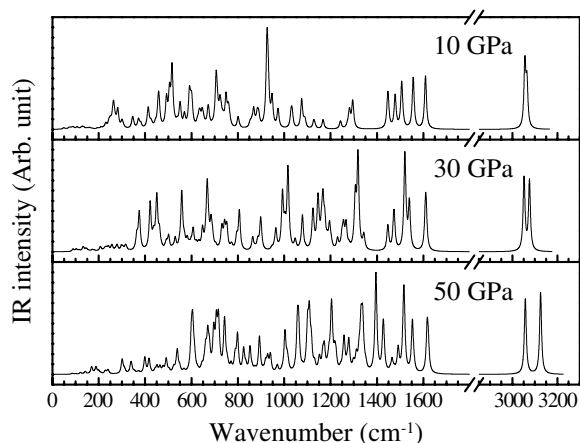


Fig. 8 IR frequencies of the AEE conformer at three pressures 10, 30, and 50 GPa obtained by MD simulations. All peaks are drawn with spectral shapes obtained by the convolution with Lorentz functions (FWHM = 10 cm⁻¹)

The pressure dependence of the IR peak positions are depicted in Fig. 8. Almost all peaks showed blue shifts as the increase of the pressures. Generally, blue shifts appear when the pressure was increased, because the high pressures make the atomic distances shorter. Calculated pressure dependence of the peak positions of the CH₂ stretching modes above 3000 cm⁻¹ are shown in Fig. 9. The patterns of the peak shifts obtained by these MD simulations were in qualitative agreement with the experimental data shown in Fig. 5. Two characteristic peak splitting patterns are similar to the experimental result. For the reason of this splitting, it is supposed that an infrared inactive vibron was changed its infrared activity caused by the molecular geometry change that was induced by the intermolecular distances decrease, in other words, by the force environment change.

5. Conclusion

FT-IR spectra of RDX were measured at various pressures from 0 to 65 GPa. A phase transition from α phase to γ phase was confirmed and pressure dependencies of the peak positions were investigated.

Although the crystal structure of high pressure phase of RDX called γ -RDX has not yet been recovered, DFT calculations and MD simulations suggested the molecular structure of γ -RDX to be AEE type. This result supports that molecular structures can change mechanochemically under high pressures. It can be said that bond stabilities change as the pressure increase.

References

- 1) D. C. Sorescu, B. M. Rice, and D. L. Thompson, *J. Phys. Chem. B* 101, 798-808 (1997).
- 2) D. C. Sorescu, B. M. Rice, and D. L. Thompson, *J. Phys. Chem. B* 102, 948-952 (1998).
- 3) D. C. Sorescu, B. M. Rice, and D. L. Thompson, *J. Phys. Chem. B* 103, 6783-6790 (1999).

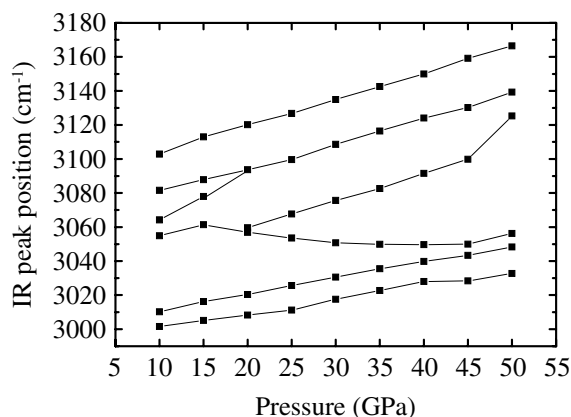


Fig. 9 Pressure dependences of the frequencies of CH₂ stretching modes of the AEE conformer obtained by MD simulations.

- 4) M. M. Kuklja, and A. B. Kunz, *J. Phys. Chem. B* 103, 8427-8431 (1999).
- 5) M. M. Kuklja, and A. B. Kunz, *J. Appl. Phys.* 87, 2215-2218 (2000).
- 6) M. M. Kuklja, E. V. Stefanovich, and A. B. Kunz, *J. Chem. Phys.* 112, 3417-3423 (2000).
- 7) M. M. Kuklja, B. P. Aduiev, E. D. Aluker, V. I. Krasheninina, A. G. Krechetov, and A. Y. Mitrofanov, *J. Appl. Phys.* 89, 4156-4166 (2001).
- 8) M. M. Kuklja, *Appl. Phys. A* 76, 359-366 (2003).
- 9) T. Luty, P. Ordon, and C. J. Eckhardt, *J. Chem. Phys.* 117, 1775-1785 (2002).
- 10) N. J. Harris, and K. Lammertsma, *J. Am. Chem. Soc.* 119, 6583-6589 (1997).
- 11) B. M. Rice, and C. F. Chabalowski, *J. Phys. Chem. A* 101, 8720-8726 (1997).
- 12) E. F. C. Byrd, G. E. Scuseria, and C. F. Chabalowski, *J. Phys. Chem. B* 108, 13100-13106 (2004).
- 13) W. F. Perger, *Chem. Phys. Lett.* 368, 319-323 (2003).
- 14) R. Hultgren, *J. Chem. Phys.* 4, 84 (1936).
- 15) C. S. Choi, and E. Prince, *Acta Cryst. B* 28, 2857-2862 (1972).
- 16) R. J. Karpowicz, and T. B. Brill, *J. Phys. Chem.* 88, 348-352 (1984).
- 17) V. Schettino, and R. Bini, *Phys. Chem. Chem. Phys.* 5, 1951-1965 (2003).
- 18) H. K. Mao, P. M. Bell, J. W. Shaner, and D. J. Steinberg, *J. Appl. Phys.* 49, 3276-3283 (1978).
- 19) G. W. Trucks, H. B. Schlegel, G. E. Scuseria, M. A. Robb, J. R. Cheeseman, J. A. Montgomery, Jr., T. Vreven, K. N. Kudin, J. C. Burant, J. M. Millam, S. S. Iyengar, J. Tomasi, V. Barone, B. Mennucci, M. Cossi, G. Scalmani, N. Rega, G. A. Petersson, H. Nakatsuji, M. Hada, M. Ehara, K. Toyota, R. Fukuda, J. Hasegawa, M. Ishida, T. Nakajima, Y. Honda, O. Kitao, H. Nakai, M. Klene, X. Li, J. E. Knox, H. P. Hratchian, J. B. Cross, C. Adamo, J. Jaramillo, R. Gomperts, R. E. Stratmann, O. Yazyev, A. J. Austin, R.

- Cammi, C. Pomelli, J. W. Ochterski, P. Y. Ayala, K. Morokuma, G. A. Voth, P. Salvador, J. J. Dannenberg, V. G. Zakrzewski, S. Dapprich, A. D. Daniels, M. C. Strain, O. Farkas, D. K. Malick, A. D. Rabuck, K. Raghavachari, J. B. Foresman, J. V. Ortiz, Q. Cui, A. G. Baboul, S. Clifford, J. Cioslowski, B. B. Stefanov, G. Liu, A. Liashenko, P. Piskorz, I. Komaromi, R. L. Martin, D. J. Fox, T. Keith, M. A. Al-Laham, C. Y. Peng, A. Nanayakkara, M. Challacombe, P. M. W. Gill, B. Johnson, W. Chen, M. W. Wong, C. Gonzalez, and J. A. Pople M. J. Frisch, Gaussian 03 Gaussian, Inc., Wallingford CT (2004).
- 20) M. W. Wong, Chem. Phys. Lett. 256, 391-399 (1996).
- 21) J. D. Gale, J. Chem. Soc. Faraday T. 93, 629-637 (1997).
- 22) S. Ye, K. Tonokura, and M. Koshi, Sci. Tech. Energetic Materials 64, 201-207 (2003).
- 23) S. J. Weiner, P. A. Kollman, D. T. Nguyen, and D. A. Case, J. Comput. Chem. 7, 230-252 (1986).
- 24) P. J. Miller, S. Block, and G. J. Piermarini, Combust. Flame 83, 174-184 (1991).
- 25) M. Rey-Lafon, C. Trinquocoste, R. Cavagnat, and M. Forel, J. Chim. Phys. PCB. 68, 1533-1542 (1971).

RDXの高圧相

後藤直之*, 山脇 浩**, 若林邦彦***, 中山良男***, 吉田正典***, 越 光男*

高感度爆薬の一種であるRDX (hexahydro-1,3,5-trinitro-1,3,5-triazine) についてダイヤモンドアンビルセル (DAC) を用いて50 GPa程度までの静的超高圧力を印加し, FT-IR分光法を用いてその振る舞いを検討した。また, RDXの6種の異性体に関してBecke3-Lee-Yang-Parr (B3LYP) 混合密度汎関数及び6-31G (d), 6-311+G (d,p), 6-311++G (3df,3pd) の基底系を用いた密度汎関数理論 (DFT) による量子化学計算を行った。FT-IRスペクトルとDFT計算を比較することによってRDXの高圧相 (γ -RDX) の分子構造を考察した。さらに, この異性化の妥当性を評価するためにポテンシャルエネルギー計算を行った。また, 赤外振動数の圧力依存を議論するために分子動力学 (MD) 計算を行った。

高圧力下におけるFT-IRスペクトルには, C_{3v} 点群の特徴である縮退した構造が現れなかった。FT-IRスペクトルと密度汎関数法 (DFT) によって計算された赤外振動数及びMD計算の結果得られた赤外振動数の圧力依存を比較すると, 高圧力下におけるRDXの分子構造はAEE型 (6員環に対してNO₂が1つは軸結合, 他の2つは赤道結合) であると考えられる。構造転移に関するポテンシャルエネルギー面の計算結果もこの結論を支持するものとなった。

*東京大学大学院工学系研究科化学システム工学専攻 〒113-8656 東京都文京区本郷7-3-1
†corresponding author: goto@chemsys.t.u-tokyo.ac.jp

**独立行政法人産業技術総合研究所計測フロンティア研究部門 〒305-8565 茨城県つくば市東1-1-1

***独立行政法人産業技術総合研究所爆発安全研究センター 〒305-8565 茨城県つくば市東1-1-1